Chapter 12
Control of Pneumatic Transport

Abstract This chapter looks at the control of pneumatic conveying systems in an effort to improve their reliability and operability. Some classic control theory is recalled as well as the topic of system stability when operating close to the unsteady regimes of choking and saltation. Some topics in artificial intelligence are cited.

Keywords Stability · Transport lags · Transfer function · Choking · Saltation · Liapunov analysis · Artificial intelligence

12.1 Basic Material Flow and Control Theory

For pneumatic transport the basic principle of analysis is the material balance of the solids transported. A number of different situations could arise for the control of the solids flow. The macro approach to the control analysis will be considered first; then more detailed distributed models of the actual solids flow will be explored.

The simplest analogue of flow of solids is to compare the system to an equivalent liquid situation. Figure 12.1 shows an input–output situation from a solids storage tank. In pneumatic transport one is probably concerned in delivering a constant outflow of mass. If m_s is the amount of solids in the storage or feeder unit then one can write.

$$\frac{dm_s}{dt} = \dot{m}_{s\alpha} - \dot{m}_{s\omega} \tag{12.1}$$

where α and ω refer to initial and terminal states respectively.

A method of maintaining the output constant is to set up a reference level in the feeder and maintain the tank pressure constant. The level or amount of solids in the tank can be continuously measured:

$$\varepsilon' = m_{sref} - m_s \tag{12.2}$$

where m_{sref} is the reference amount of solids in the tank. The error can be set proportional to the inlet flow of solids so that

$$\dot{m}_{s\alpha} = K\varepsilon' \tag{12.3}$$

G.E. Klinzing et al., *Pneumatic Conveying of Solids: A Theoretical and Practical Approach*, Particle Technology Series 8, DOI 10.1007/978-90-481-3609-4_12,

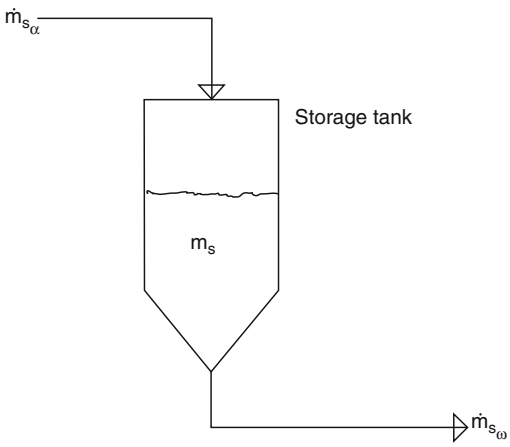

Fig. 12.1 Input/Output from a storage tank

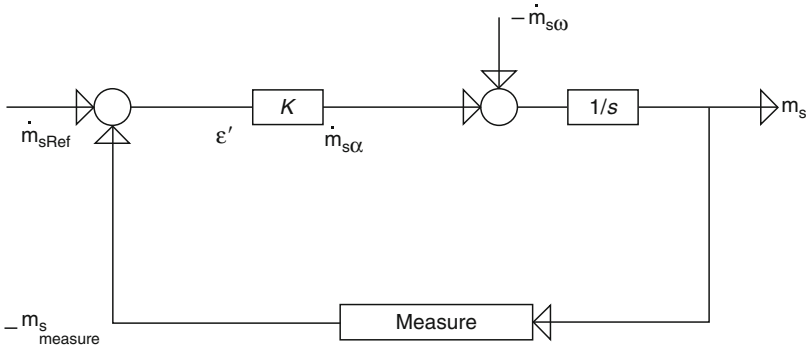

Fig. 12.2 Control block diagram for a storage tank

This is only one type of control that can be employed. Various control schemes can be incorporated at this point in the analysis. The basic differential Eq. 12.1 is expanded to yield

$$\frac{dm_s}{dt} + Km_s = Km_{s\,ref} - \bar{\dot{m}}_{so} \tag{12.4}$$

With Laplace transforms one has

$$m_s(s) = \frac{1}{s+K}[Km_{s\,ref}(s) - \bar{\dot{m}}_{so}(s) + m_s(0)] \tag{12.5}$$

The signal-flow diagram for this case is shown in Fig. 12.2.

Another set-up that is common in pneumatic transport has a rarer analogue in the liquid systems – a blow tank arrangement. A blow tank or delivery tank with solids can be pressurized to deliver the solids into and through a pipeline.

An initial charge is placed in the tank. Figure 12.3 shows this arrangement. The balance of solids can be written as

$$\frac{dm_s}{dt} = -\dot{m}_{s\omega} \tag{12.6}$$

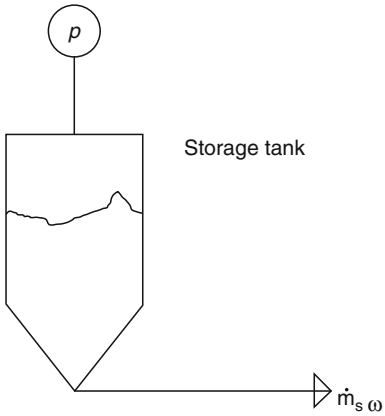

Fig. 12.3 Blow tank diagram

If one measures the output flow rate continuously as can be done with modern flow devices, an error signal can be set up as

$$\varepsilon = \dot{m}_{s\alpha ref} - \dot{m}_{s\omega} \tag{12.7}$$

The outflow of mass from the tank is dependent on the amount of mass in the unit and the applied pressure. Using a linear combination for this phenomenon one has

$$\dot{m}_{s\omega} = \alpha m_s + \beta p_{tank} \tag{12.8}$$

The pressure in the tank can be related to the error signal by a proportional control such that

$$p_{tank} = K(\dot{m}_{pref} - \dot{m}_{p\omega}) \tag{12.9}$$

Combining the above expressions one has

$$\frac{dm_s}{dt} = -[\alpha m_s + \beta K(\bar{\dot{m}}_{p\varpi ref} - \bar{\dot{m}}_{p\omega})] \tag{12.10}$$

Applying Laplace transforms one finds

$$m_s(s) = \frac{1}{s+\alpha}[m_s(0) - \beta K(\bar{\dot{m}}_{s\omega ref}(s) - \bar{\dot{m}}_{s\omega}(s))] \tag{12.11}$$

The signal-flow diagram for this control is shown in Fig. 12.4. Note that s is Laplace transform notation.

12.2 Transport Lags

The movement of the solids through a line can produce a lag time in the process. This transport of course is the very essence of pneumatic conveying. The lag time Δt can be represented as distance of the transport line divided by the solids velocity,

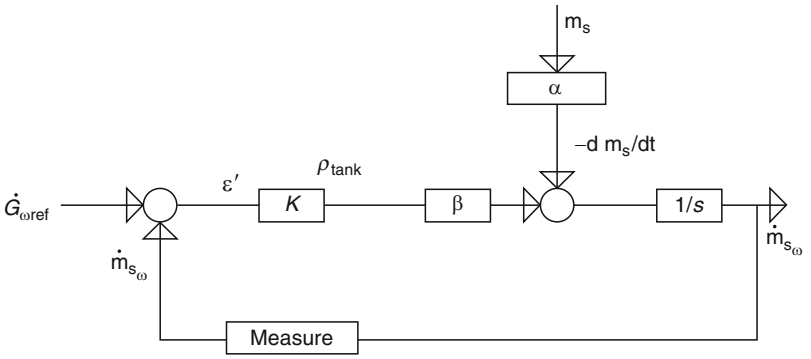

Fig. 12.4 Control block diagram for a pneumatic conveying line

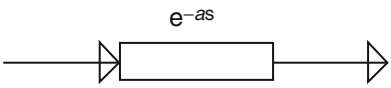

Fig. 12.5 Lag for a conveying line

L/c. In describing the process in the form of a signal-flow diagram (Fig. 12.5) the term e^{-as} in the Laplace transform format must be added for the lag time term. The constant a depends on the details of the solids movement in a given line. In the signal-flow format one has inserted the lag time term before the 1/s terms. One should note that screw conveyors can also be represented in the same lag format.

12.3 Analysis of Gas–Solid Flow by Transfer Functions

Pneumatic transport systems can be analysed by transfer functions if the process described is of first order. The analysis can begin by considering a driving force pressure drop as

$$p_\alpha - p_\omega = p_{in} - p_{out} \tag{12.12}$$

At steady state this driving force is balanced by the frictional (f), gravitational (g) and electrostatic (el) forces present in the system; thus

$$p_\alpha - p_\omega = \Delta p_f + \Delta p_g + \Delta p_{el} \tag{12.13}$$

For the unsteady state the balance must be modified with Newton's second law as [1]

$$V\frac{dv}{dt} + m_s\frac{dc}{dt} = A(p_\alpha - p_\omega) - A(\Delta p_f + \Delta p_g + \Delta p_{el}) \tag{12.14}$$

where V is the mass of fluid in the line and m_s is the mass of solids in the line. If a valve or bend is in the line, these pressure losses can be added to the above equation.

One now inserts a perturbation into the above variables. The variable will be composed of a steady state value and a fluctuating component:

$$\begin{aligned} p_\alpha &= p_\alpha + p_{in}^1 \\ p_\omega &= p_\omega + p_{out}^1 \\ \Delta p_f &= \Delta p_f + \Delta p_f^1 \\ \Delta p_g &= \Delta p_g + \Delta p_g^1 \\ v &= v + v^1 \\ c &= c + c^1 \end{aligned} \tag{12.15}$$

Inserting these definitions into Eq. 2.14 one obtains

$$m_f \frac{dv^1}{dt} + m_s \frac{dc^1}{dt} = (p_\alpha^1 - p_\omega^1) - A(\Delta p_f^1 + \Delta p_g^1) \tag{12.16}$$

since

$$\bar{p}_\alpha - \bar{p}_\omega = \Delta\bar{p}_f + \Delta\bar{p}_g$$

The Laplace transform can now be taken from Eq. 12.16:

$$\begin{aligned} &m_f\left[sv(s) - v^1(0)\right] + m_s\left[sc(s) - c^1(0)\right] \\ &\quad = A\left[p_\alpha^1(s) - p_\omega^1(s)\right] - A\left[\Delta p_f^1(s) + \Delta p_g^1(s)\right] \end{aligned} \tag{12.17}$$

A number of different assumptions can be employed at this point to develop the specific transfer functions.

Setting $v^1(0)$ and $c^1(0)$ equal to zero and the gravity fluctuations term as negligible one has

$$m_f sv(s) + m_s sc(s) = A\left[p_\alpha^1(s) - p_\omega^1(s)\right] - A\left[\Delta p_f^1(s)\right] \tag{12.18}$$

If the gas velocity fluctuation is smaller than the particle velocity and the frictional fluctuation is dominated by the particle fluctuation, one can write

$$m_s sc(s) = A[p_\alpha^1(s) - p_\omega^1(s)] - A\left(\frac{\partial(\Delta p_f)}{\partial c}\right) c(s) \tag{12.19}$$

Solving for c(s)

$$c(s) = \frac{A\left[p_\alpha^1(s) - p_\omega^1(s)\right]}{m_s s + A\partial(\Delta p_f)/\partial c} \tag{12.20}$$

Letting $\Delta p_T^1 = p_{in}^1(s) - p_{out}^1(s)$

$$\frac{c(s)}{\Delta p_T^1} = \frac{A^{-1}\partial c/\partial(\Delta p_f)}{1 + m_s s/A(\partial(\Delta p_f)/\partial c)} = \frac{K}{1 + \tau s} \tag{12.21}$$

Thus from transfer analysis the time constant is

$$\tau = \frac{m_s/A}{\partial(\Delta p_f)\partial c} \tag{12.22}$$

and the gain is

$$K = \frac{1}{A}\left(\frac{\partial c}{\partial(\Delta p_f)}\right) \tag{12.23}$$

The term $\partial(\Delta p_f)/\partial c$ can be written in terms of the friction factor with

$$\Delta p_f = \lambda_Z^* \rho_p (1-\varepsilon)\frac{c^2}{2}\frac{L}{D} \tag{12.24}$$

Now taking the derivative gives

$$\frac{\partial(\Delta p_f)}{\partial c} = \lambda_Z^* \frac{\rho_p}{D} cL(1-\varepsilon) \tag{12.25}$$

Resubstituting these terms into the time (response time) constant and gain factor for changes in input with some simplifications, such as $m_s = LA(1-\varepsilon)\rho_p$,

$$\tau = \frac{D}{\lambda_Z^* c} \tag{12.26}$$

$$K = \frac{4}{\pi \lambda_Z^* c \rho_p (1-\varepsilon) LD} \tag{12.27}$$

Thus the response time of a gas–solid system can be estimated in the above fashion.

12.4 Stability of Pneumatic Transfer Systems

The question of how stable a pneumatic transfer system is, is often posed when design of a new arrangement or modification in existing units is made. The word stable may mean simply that a small perturbation in the line pressure and velocity will not upset the steady flow condition enough to cause the system to change to a choking flow condition. Leung, Wiles and Nicklin [2] and Doig [3] were the first to consider such an excursion of gas–solid flows. They were interested in the coupling of a blower and a transport line and how one unit interacted with the other. Figure 12.6 shows a plot of the blower curve on the gas–solid pressure drop–velocity phase diagrams. A perturbation in the pressure drop caused by a sudden blockage of the line can drive the flow from point (c) to (b) and then to point (a) which is located near the dangerous choking regime. The coupling of such blower and transport lines is not to be taken lightly for stable pneumatic transport operations. Chapter 6 has more detail on this subject.

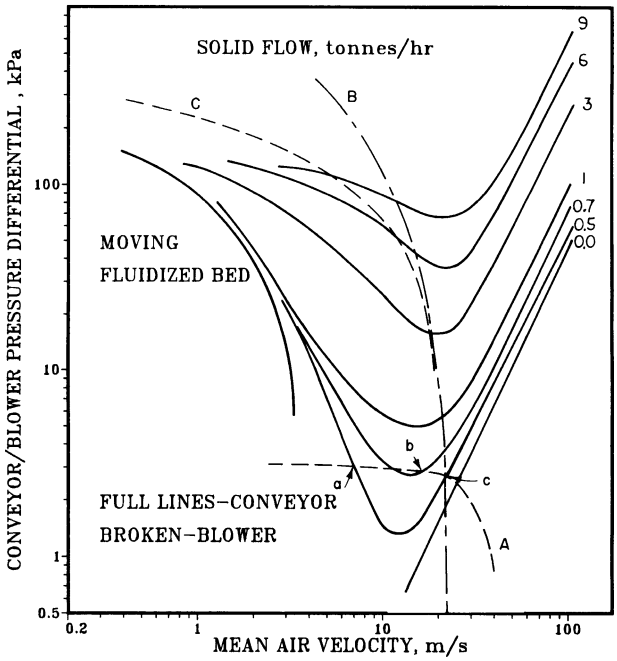

Fig. 12.6 Phase diagram with a blower performance overlay

Another way of viewing stability is to investigate the basic gas and solid equations describing pneumatic transport and then to apply standard mathematical analysis to probe the conditions of stability. The essential part of such an analysis is to be able to relate this mathematical stability back to physical phenomena occurring in actual pneumatic systems. In an effort to explore this important aspect of pneumatic transfer two linear approaches will be considered along with one non-linear analysis.

12.5 Air Control Systems for Pneumatic Conveying Systems

According to the state diagram for a specific pneumatic conveying system, the air control system has to set a certain air flow rate. Even systems with different routing – going either to the first or last silo of a large farm – or different flow rates – recirculation at higher capacity than transfer to bagging – may require the identical air flow rate for pneumatic conveying. Such examples exist especially in dense phase conveying applications in the petrochemical and plastics industry.

The easiest way to set a respective constant flow rate from a plant air supply net is to use a Laval nozzle. Within the smallest cross-section of the Laval nozzle, the velocity of sound will be achieved as long as the absolute pressure downstream

from the Laval nozzle, i.e., the conveying pressure, does not exceed approximately 80% of the upstream pressure. With the velocity of sound depending only on the gas properties and the temperature, the flow rate can easily be calculated from the Laval nozzle cross-section, the temperature and the gas density at the upstream pressure.

Varying air flow rates can be achieved by installing a pressure control valve (regulator) upstream from the Laval nozzle and thus adjusting the air flow rate by varying the gas density due to different pressures. This system, however, has the disadvantage of lowering the available conveying pressure when reducing the air flow rate. Thus, the ultimate solution is an adjustable Laval nozzle, as recently introduced by Wilms [4]. This Laval nozzle has a slotted cross-section with varying slot width or height. Thus, the geometric requirements for the opening angle remain constant.

Dense phase conveying systems require cleaning of the line prior to any product or grade change in order to prevent cross-contamination of different product qualities. Therefore, at the end of the dense phase conveying cycle, the conveying line has to be cleaned from residual product by a short time of dilute phase conveying. For this period of time, a larger air flow rate is required. Conventional systems use a separate roots blower for supply of this additional air flow rate. An alternative is to use the energy of the highly compressed air from the dense phase conveying system (approximately 45–50 psig) to drive an ejector. This ejector then sucks the additionally required air flow rate via an inlet filter from the environment. This system works since line cleaning needs a high gas velocity, but only a small pressure, because there is only a small amount of solids still to be conveyed through the system.

Thus, the ultimate air control system will use an adjustable Laval nozzle for supply of the conveying air flow rate and an ejector for line cleaning purposes. Regarding the control system, application of an adjustable Laval nozzle can optimize the system throughout by setting the rotary feeder speed in relation to the conveying pressure. If shorter line routes are being used, then a higher capacity can be achieved on this route. A typical example is the recirculation of pellets to the top of a blender with a much higher solids flow rate than the transfer rate to the bagging system which is several hundred feet further away.

12.6 Stability Analysis with Taylor Series Linearization

The basic dynamic equations for this stability analysis are the same as Eqs. 4.25 and 4.26. The non-linear terms in these equations deal with the slip velocity and velocity of the fluid or particle in a squared format. The Taylor series linearization will be applied to these terms in an expansion around the steady state velocities. For example,

$$(v - c)^2 \approx (v^* - c^*)^2 + 2(v^* - c^*)(v - c - v^* + c^*) \tag{12.28}$$

where the velocity can be broken into a steady and a fluctuatory component $c = c^* + \tilde{c}$ and $v = v^* + \tilde{v}$.

Employing these expansions in the dynamic equation one obtains finally the transformed linear system

$$\frac{d\tilde{c}}{dt} = \alpha_0 + \alpha_1\tilde{c} + \alpha_2\tilde{v} \tag{12.29a}$$

$$\frac{d\tilde{v}}{dt} = \beta_0 + \beta_1\tilde{c} + \beta_2\tilde{v} \tag{12.29b}$$

which upon combination will yield a second-order differential equation

$$\frac{d^2\tilde{c}}{dt} = \gamma_1\frac{d\tilde{c}}{dt} + \gamma_2\tilde{c} + \gamma_3 \tag{12.30}$$

Analysis for the stability of Eq. 12.30 involves simply finding the region in which the eigenvalues of the solutions go positive, showing a growth factor and thus instability. The eigenvalues of Eq. 12.30 are easily expressed as

$$m = \frac{-\gamma_1 \pm (\gamma_1^2 - 4\gamma_2)^{1/2}}{2} \tag{12.31}$$

The constants in the above equations can be shown as

$$\gamma_1 = +(\alpha_1 + \beta_2)$$
$$\gamma_2 = (+\alpha_2\beta_1 - \alpha_1\beta_2)$$
$$\gamma_3 = \alpha_2\beta_0 - \alpha_0\beta_2$$

and

$$a_0 = -\frac{1}{\rho_p}\frac{dp}{dx} - g + \frac{3C_{DS}\varepsilon^{-4.7}}{4d}\frac{\rho_f}{\rho_p}[-(v^* - c^*)]^2$$
$$- \frac{\lambda_Z^*}{2D}\begin{Bmatrix} -c^{*2} \\ -(v^* - c^*)^2 \end{Bmatrix}\begin{matrix} \text{squared format} \\ \text{slip format} \end{matrix}$$

$$a_1 = \left\{\frac{3C_{DS}\varepsilon^{-4.7}}{4d}\frac{\rho_f}{\rho_p}[2(v_s^* - c*)]\right\}$$
$$- \frac{\lambda_Z^*}{2D}\begin{Bmatrix} c^{*2} \\ 2(v^* - c^*)^2 \end{Bmatrix}\begin{matrix} \text{squared format} \\ \text{slip format} \end{matrix}$$

$$\alpha_0 = a_0; \alpha_1 = -(a_1 + a_2); \alpha_2 = a_1 + a_2$$

and

$$b_0 = -\frac{1}{\rho}\frac{dp}{dx} - g + \frac{3C_{DS}\varepsilon^{-4.7}}{4d}\frac{1-\varepsilon}{\varepsilon}[-(v^* - c^*)^2] - \frac{2f_L}{D}(v^{*2})$$

$$b_1 = +\frac{3C_{DS}\varepsilon^{-4.7}}{4d}\frac{1-\varepsilon}{\varepsilon}[2(v^* - c^*)]$$

$$b_2 = \frac{-2F_L}{D}(2v^*)$$
$$\beta_0 = b_0; \beta_1 = -b_1; \beta_2 = (b_1 + b_2)$$

One will note that for the α parameters two choices are given as to the frictional representations for the solid friction factors. The first is a particle velocity format such as that of Konno and Saito [5] while the second is a slip velocity representation.

Exploring the eigenvalues of Eq. 12.30 shows that positive eigenvalues are generated to the left of the minimum point on the pressure drop with velocity curve at constant solids flow. This is the region experimentally that shows a sharp increase in pressure drop moving toward a choking condition. This linearization process has served to describe the basic characteristics of the gas–solid flow system.

12.7 Linear Stability Analysis: Jackson Approach

The second linear stability analysis to be discussed is one that has been pioneered by Jackson [6] for fluidization and adopted by Grace and Tuot [7] for pneumatic transport. The approach of Jackson considers the continuity equations for the solids and the gas along with the dynamic equation of the solids alone. The dynamic equation of the solids does not include the pressure drop term. Defining the velocity and number density perturbation as

$$v = v^* + \tilde{v}$$
$$c = c^* + \tilde{c}$$
$$n = n_0 + \tilde{n}$$

and inserting these into the continuity and dynamics equation and ignoring all but the first-order terms, one obtains

$$\nabla.\tilde{v} = \frac{c}{1 - n_0 c}\left(\frac{\partial \tilde{n}}{\partial t} + v^* \nabla \tilde{n}\right) \tag{12.32}$$

$$\begin{aligned} \nabla.\tilde{c} = &-\frac{1}{n_0}\left(\frac{\partial \tilde{n}}{\partial t} + c^* \nabla \tilde{n}\right) \\ &\times n_0 m_s \left(\frac{\partial \tilde{c}}{\partial t} + c^* \frac{\partial \tilde{c}}{\partial x}\right) - n_0 \rho c^* \left(\frac{\partial \tilde{v}}{\partial t} + v^* \frac{\partial \tilde{v}}{\partial x}\right) \\ &+ g\tilde{n}(m_s - \rho c^*) - \beta_0(\tilde{v} - \tilde{c}) - \tilde{n}\beta_0^1(v^* - c^*) \\ &= 0 \end{aligned} \tag{12.33, 12.34}$$

In Eq. 12.34

$$\beta_0 = (1 - \varepsilon)\frac{(\rho_p - \rho)g}{(v^* - c^*)} \tag{12.35}$$

The procedure involves using the function

$$\tilde{n} = f(t)\exp[i(k_x)] \tag{12.36}$$

to be inserted in Eqs. 12.31, 12.32 and 12.33 to produce a second order differential equation in f(t) whose solution produces again two eigenvalues defined as

$$s_1, s_2 = \frac{b}{2a}\left\{\pm[1 + 4(\alpha - 1)(C^2/b^2) - 4i(C/b)(ae - 1)]^{1/2} - [1 + 2i(C/b)(1 + q)]\right\} \tag{12.37}$$

where,

$a = 1 + \rho_p\varepsilon/\rho(1 - \varepsilon)$
$b = \rho_p - \rho(1 - \varepsilon)(v^* - c^*)$
$C = k(v^* - c^*)$
$e = 1 - 2\varepsilon + \varepsilon n_0\beta_0^1/\beta_0$
$q = c^*a(v^* - c^*)$

For stability the growth term in distance is given as

$$\Delta x = \mathrm{Im}(s_1)/k\,\mathrm{Re}(s_1) \tag{12.38}$$

Interpretation is understood by the concept that the smaller the positive values of Δx are the easier the system becomes in its ability to form clusters of particles indicating instability. In this analysis one notes that

$$k = \pi/50d \quad \frac{n_0\beta_0'}{\beta_0} = \frac{(\eta - 1) - \varepsilon_s(\eta - 2)}{\varepsilon_s}$$

where $\eta = 4.7$ by Richardson and Zaki and $\varepsilon_s = 0.43$ for a packed bed. Table 12.1 shows some values for the growth distance Δx for typical systems; the larger Δx the more stable the system.

Joseph, Larourre and Klinzing [8] have employed this analysis to explore the effect of electrostatic forces on the stability of pneumatic transport. They found the electrostatic forces decreased the growth distances thus indicating a less stable system.

Table 12.1 Growth distances (Δx(m)) for 100 μm particles with air at 6 m/s

			ε			
T (K)	P (K Pa)	ρ_p (kg/m^3)	0.7	0.8	0.9	0.98
300	101	7,800	0.144	0.152	0.190	0.43
300	101	2,600	0.21	0.20	0.26	0.73
1,300	101	2,600	0.53	0.35	0.39	1.55
300	101	480	3.4	1.62	1.62	12.4

12.8 Stability via the Liapunov Analysis

The former analyses considered stability of gas–solids flows from the linearization aspect. The results which have been obtained in this fashion appear to agree adequately with the experimental findings especially in the phase plane analysis. To include the non-linear terms in the analysis would generally require a numerical solution with graphical interpretation of the findings. In the area of stability analysis in other fields of endeavour the second method of Liapunov stands out as a technique of great utility. Not only are the non-linear terms able to be handled in this technique but also regions of stability can be established without great computational difficulties. The second method of Liapunov is based on a generalization of the idea that if a system has an asymptotically stable equilibrium state then the stored energy of the system displaced with a region of attraction decays with increasing time until it finally assumes its minimum value at the equilibrium state.

The idea of a Liapunov function is more general than that of energy and is far more widely applicable. The Liapunov functions are functions of independent variables $V_1, \ldots, V_n$ and t and can be denoted as V(y, t) or V(y) if t is not explicit. The sign of the function V(y) and its time derivative $\dot{V}(y)$ give information about the stability, asymptotic stability or instability of the equilibrium state under study without directly solving for the detailed solution.

Global asymptotic stability can be guaranteed for a system if it is possible to formulate a scalar function (the Liapunov function) with continuous first partial derivatives such that:

$$\begin{aligned} &\text{(a) } V(y) = 0, y = 0 \\ &\text{(b) } V(y) > 0, y = 0 \\ &\text{(c) } V(y) \to \infty, \|y\| \to \infty \\ &\text{(d) } \dot{V}(y) = dV/dt < 0, y \neq 0 \end{aligned} \tag{12.39}$$

LaSalle and Lepchetz [9] have shown that if conditions (a), (b) and (d) are satisfied within a bounded region defined by $V(y) < C$, where C is some positive constant, then the system is asymptotically stable in that bounded region.

A possible Liapunov function is the quadratic form

$$V = y^T p_y \tag{12.40}$$

where p in a two-dimensional system is a matrix

$$\begin{bmatrix} p_{11} & p_{12} \\ p_{21} & p_{22} \end{bmatrix}$$

If p is chosen as the identity matrix, then the Liapunov function is merely the norm of the state vector y. The basic gas–solids equations given by Eqs. 4.25 and 4.26 can serve as the basic starting point for this analysis. One transformation is necessary to

form a system of equations in which the steady state has a vector coordinate of zero. This is achieved by the following transforms:

$$\tilde{c} = c - c^* \tag{12.41}$$

$$\tilde{v} = v - v^* \tag{12.42}$$

where c^* and v^* are the steady state solutions of Eqs. 4.25 and 4.26. It should be noted that the pressure drop is assumed constant in this analysis. In the new system the equations can be written as

$$\frac{d\tilde{c}}{dt} = \frac{3}{4}\frac{C_{DS}}{d}\frac{\rho}{\rho_p - \rho}[(\tilde{v} + v^*) - (\tilde{c} + c^*)]^2 - g - \frac{1}{\rho_p}\frac{\partial p}{\partial x} - \frac{\lambda_Z^*}{2D}(\tilde{c} + c^*)^2 \tag{12.43}$$

$$\frac{d\tilde{v}}{dt} = \frac{3}{4}\frac{C_{DS}\rho}{d(\rho_p - \rho)}[(\tilde{v} + v^*) - (\tilde{c} + c^*)]^2 - \frac{\lambda_Z^*}{2D}(\tilde{v} + v^*)^2 - \frac{1}{\rho}\frac{\partial p}{\partial x} \tag{12.44}$$

The Liapunov function which is taken to be the norm of the state vector is

$$V(U) = \tilde{v}^2 + \tilde{c}^2 \tag{12.45}$$

and

$$\frac{dV}{dt} = 2\tilde{v}\frac{d\tilde{v}}{dt} + 2\tilde{c}\frac{d\tilde{c}}{dt} < 0 \tag{12.46}$$

The above equations can be substituted in this equation in order to define the boundary between the regions of stable and unstable conditions. One sets $dV/dt = 0$ and solves for the resultant cubic equation for c at varying values of v. By doing this while varying one system parameter such as particle size, density etc. it is possible to assess the effect of that parameter on the shape and size of the region of stability. Figure 12.7 shows a typical result of the application of the Liapunov method to gas–solids flow. The figure shows increasing circles of stability as the flow increases in the phase plane $\Delta p/L$ versus v at a constant $\dot{m}_p$. One finds the centre of the circle as the steady state solution. If a perturbation exists in the system and the perturbation does not violate the circle's boundary, the system will return to the steady state when the perturbation is removed. If the perturbation crosses the circle's boundary, the system can go to another steady state or become unstable if it crosses the stability boundary line. There are certain limitations to the Liapunov second method that must be mentioned:

(a) The stability conditions obtained from a particular v function are sufficient but may not be necessary to ensure stability.
(b) Failure to find a V function can give no information on stability conditions.
(c) Although a particular V function may prove that the equilibrium state under consideration is stable in a region which includes this equilibrium state, it does not necessarily mean that the motions outside this region are unstable.

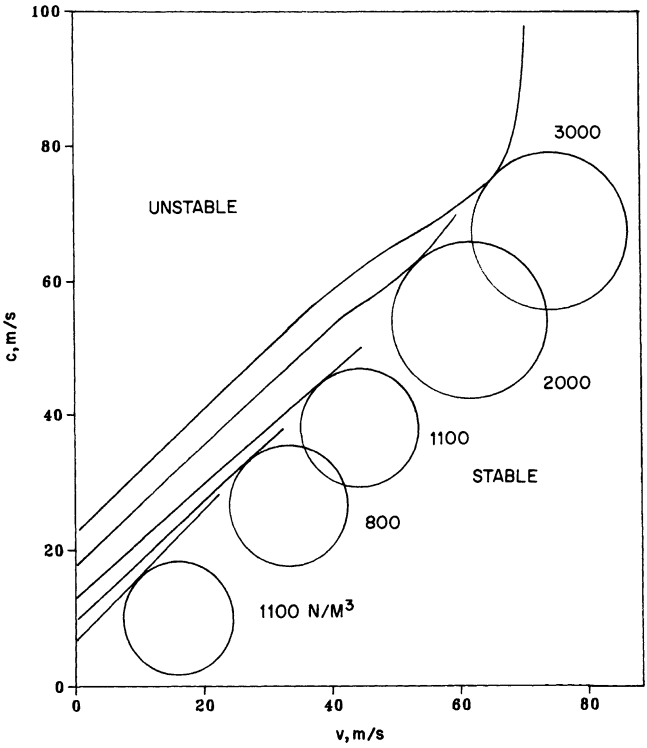

Fig. 12.7 Liapunov stability diagram

12.9 Artificial Intelligence and Solids Processing

Artificial intelligence has several different aspects that lends itself to applications in the area of pneumatic conveying and solids processing in general. One can use the expert system approach to capture information from the literature and experts alike to develop a set of rules that can handle such questions as: What is the best pneumatic conveying system for my applications? Shall I use a pressure or vacuum conveying? Shall I explore dense phase transport? Klinzing and his associates [10–13] have developed a package called NUSELECT just to answer such questions. To try to decide which is the best feeder for a conveying operation, the engineer is presented with many options, several of which will be fine while others will be problematic. One cannot go to a series of equations to make such decisions; however, expert systems are ideal for such decisions and Klinzing's group has developed the program FEEDER for this purpose. To complete the expert system approach to analysis on pneumatic conveying system a program called PANACEA has been developed to address trouble shooting a particular system. The program extracts information from the users, trying to diagnose the cause of the difficulty. At some points the user is asked to run the system and report back the findings.

The field of expert systems offers a wide variety of help to the practising engineer faced with day-to-day problems in conveying. These systems coupled with programs to determine the pressure losses and flow rates can provide an effective package to address most pneumatic conveying operations.

Another type of artificial intelligence that has been great potential in pneumatic conveying is neural networking. This procedure mimics the way that the brain processes information relying on the parallel process procedure. The technique offers, in addition to a new approach, speed in processing large amounts of information. The information that is fed into a neural network is first used to train the neural network to recognize known solutions from known conditions. The more information that we can use to train the net, the more accurate the final result. Neural networks consist of numerous single units called processing elements. The collective whole of these units is the key to the application. Processing elements for neural networks exist at three levels; input level, hidden level and output level. A common way to interconnect these levels or layers is back-propagation. The neural network can function with new data after it has been trained and it can also update its knowledge as newer situations are encountered. This process gives the technique tremendous potential to address problems such as identification of various flow regimes in pneumatic conveying. In addition, one can couple the field of control into the neural net process giving one the opportunity to correct operating conditions on-line so that systems will not fail.

Another avenue in artificial intelligence is the use of fuzzy logic. Fuzzy logic has been available since 1965 but is now used for many applications from home products such as washing machines to complex production plants. This procedure considers

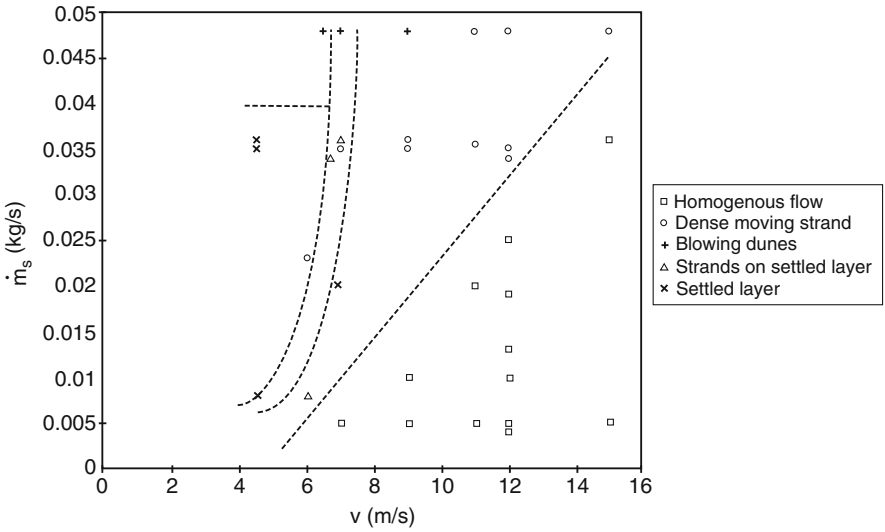

Fig. 12.8 Solids flow rate versus gas velocity for pneumatic conveying depicted in a flow map for fuzzy analysis

such terms as ‘like’, ‘almost’, ‘good’, ‘better’, ‘best’, ‘mostly’, ‘at times’, etc. and applies a mathematical technique to quantify them. These types of terms often arise in pneumatic conveying and solids processing. Using observations and data from pneumatic conveying systems, different flow patterns were addressed from a simple plot of solids flow rate versus the gas velocity. The regimes are marked according to the flow pattern observed at these points. Division lines are inserted by the user. The closer to the line the fuzzier or more unsure is the user of the actual condition. The further the operating point is from a demarcation line the surer the flow pattern. This information can also be used in a control strategy for pneumatic conveying. Figure 12.8 shows one such fuzzy map.

References

1. Weber, T.W.: An Introduction to Process Dynamics and Control. Wiley, New York (1973)
2. Leung, L.S., Wiles, R.I., Nicklin, D.J.: Ind. Eng. Chem. Process Design Development **10**, 183 (1971)
3. Doig, I.D.: S. African Mech. Eng. **25**, 394 (1975)
4. Wilms, W.: Pneumatic Conveying Symposium – Powder Technology Forum, AIChE, Denver, CO, August (1994)
5. Konno, H., Saito, S.J.: Chem. E. Japan **2**, 211 (1969)
6. Jackson, R.: Trans. I. Chem. E. **41**, 13 (1963)
7. Grace, J.R., Tuot, J.: Trans. I. Chem. E. **57**, 49 (1979)
8. Joseph, S., Larourre, P.J., Klinzing, G.E.: Powder Technol. **38**, 1 (1984)
9. LaSalle, J., Lepchetz, S.: Stability by Liapunov’s Direct Method with Applications. Academic, New York (1981)
10. Dhodapkar, S.V., Klinzing, G.E.: In: Roco, M. (ed.) Expert Systems in Solids Handling (Chapter 21), pp. 743–777 (1993)
11. Klinzing, G.E.: Powder Handling and Processing **6**(2), 1–5 (1994)
12. Dhodapkar, S.V., Klinzing, G.E.: Proc. 2nd World Congress of Part. Tech., pp. 69–75. Kyoto, Japan, September (1990)
13. Klinzing, G.E.: Proc. Intl. Sym. RELPOWFLO II, pp. 451–499. Oslo, Norway, August (1993)